

# High-power diode-pumped $Q$ -switched intracavity frequency-doubled Nd:YVO<sub>4</sub> laser with a sandwich-type resonator

Yung-Fu Chen

Department of Electrophysics, National Chiao Tung University, Hsinchu, Taiwan

Received April 5, 1999

A compact and efficient diode-pumped acousto-optically  $Q$ -switched intracavity frequency-doubled Nd:YVO<sub>4</sub>/KTP green laser is demonstrated. With 0.5-at. % Nd:YVO<sub>4</sub>, greater than 4.6 W of 532-nm average power at a repetition rate of 50 kHz was generated with 17-W pump power, corresponding to a conversion efficiency of 27%. At 10–30 kHz the pulse width is shorter than 10 ns, and the peak power is higher than 13 kW. © 1999 Optical Society of America

OCIS codes: 140.3480, 140.3540, 320.7090, 190.7220, 140.3580.

Many applications such as optical communications from deep-space and undersea imaging require efficient, compact, high-peak-power and high-repetition-rate (>20-kHz) visible-wavelength lasers. Diode-pumped solid-state lasers have been shown to be efficient, compact, and reliable all-solid-state optical sources. Recently developed diode-pumped pulsed visible lasers include actively and passively  $Q$ -switched intracavity frequency-doubled lasers.<sup>1–3</sup> Active  $Q$ -switching lasers have the advantage over passive techniques of greater pulse management, although this is usually at the expense of more complexity.

The sandwich-type flat–flat cavity that consists of a coated gain medium and a coated frequency doubler has been used to produce green lasers in cw mode and the passive  $Q$ -switch mode up to several hundred milliwatts per second.<sup>4,5</sup> In this Letter a high-power, high-repetition-rate  $Q$ -switched and intracavity frequency-doubled Nd:YVO<sub>4</sub> green laser with a sandwich-type resonator, as shown in Fig. 1, is described. More than 4.6 W of 532-nm average power at a repetition rate of 50 kHz was generated with 17-W pump power, corresponding to a conversion efficiency of 27%.

Nd:YVO<sub>4</sub> has often been used in diode-pumped intracavity frequency-doubled lasers because of its high absorption over a wide pumping wavelength bandwidth and its large stimulated-emission cross section at lasing wavelength. Unfortunately, however, power scaling with Nd:YVO<sub>4</sub> has been hindered by thermally induced fracture.<sup>6</sup> In a recent study,<sup>7</sup> I found that the fracture-limited pump power for an end-pumped laser is inversely proportional to the absorption coefficient; i.e.,

$$P_{\text{lim}} = \frac{1}{\alpha} \frac{4\pi R_T}{\xi}, \quad (1)$$

where  $\xi$  is the fractional thermal loading,  $\alpha$  is the absorption coefficient at the pump wavelength, and  $R_T$  is a thermal shock parameter that depends on the mechanical and thermal properties of the host material. The absorption coefficient of the laser crystal increases linearly with increasing dopant concentration. Therefore, lower concentrations of Nd<sup>3+</sup> can be beneficial in

extending the fracture-limited pump power. Here I report using Nd:YVO<sub>4</sub> crystals with different Nd<sup>3+</sup> concentrations (0.5–2.0 at. %) to investigate their output performance.

The experimental setup included a 0.8-mm-core fiber with a numerical aperture of 0.16 and a maximum output power of 20-W. The lengths of Nd:YVO<sub>4</sub> crystals were 6, 3, and 3 mm for 0.5, 1.0, and 2.0 at. % Nd<sup>3+</sup> concentrations, respectively. All crystals were  $a$  cut to yield a high-gain  $\pi$  transition. The Nd:YVO<sub>4</sub> crystal was wrapped with indium foil and mounted in a water-cooled copper block. The water temperature was maintained at 17 °C. One side of the Nd:YVO<sub>4</sub> crystal was coated to be nominally highly reflecting (HR) at both the fundamental wavelength ( $R > 99.9\%$ ) and the second-harmonic wavelength ( $R > 98\%$ ) and highly transmitting (HT) at the pump wavelength ( $T > 95\%$ ). The remaining side was antireflecting at the fundamental wavelength ( $R < 0.2\%$ ). The 20-mm-long  $Q$  switcher (Gooch and Housego) had antireflectance coatings at 1064 nm on both faces and was driven at a 41-MHz center frequency with 3.0 W of rf power. The KTP crystal was 20 mm long and coated to be nominally highly reflecting at the fundamental wavelength ( $R > 99.9\%$ ) and highly transmitting at the second-harmonic wavelength ( $T > 95\%$ ). The remaining side was antireflecting at the fundamental wavelength ( $R < 0.2\%$ ).

The thermally induced lens in the laser crystal brings the flat–flat cavity into geometrical stability. This concept was found at nearly the same time by Zayhowski and Mooradian<sup>8</sup> and by Dixon *et al.*<sup>9</sup> However,

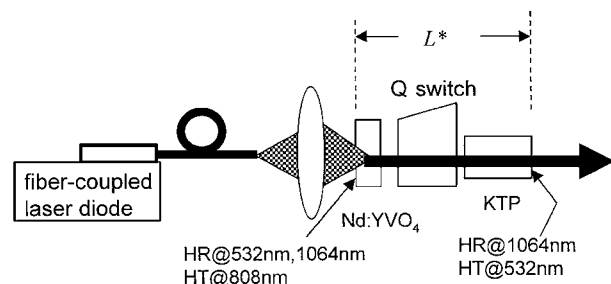


Fig. 1. Experimental setup for the  $Q$ -switched intracavity-frequency-doubled green laser.

an end-pump-induced thermal lens is not a perfect lens but is rather an aberrated lens. It has been found that the thermally induced diffraction loss at a given pump power is a rapidly increasing function of the mode-to-pump ratio. Practically, the optimum mode-to-pump ratio is in the range of approximately 0.8–1.0 when the incident pump power is greater than 5 W. The laser mode size in the present cavity is determined by the thermal lens and the effective length  $L$  of the cavity. For a fiber-coupled laser diode, the thermal lens can be given by<sup>10</sup>

$$\frac{1}{f_{\text{th}}} = \int_0^l \frac{\xi P_{\text{abs}}}{4\pi K_c} \frac{\alpha \exp(-\alpha z)}{1 - \exp(-\alpha l)} \frac{(dn/dT + n\alpha_T)}{\omega_p^2(z)} dz, \quad (2)$$

where  $K_c$  is the thermal conductivity,  $P_{\text{abs}}$  is the absorbed pump power,  $n$  are the refractive indices along the  $c$  axis of the Nd:YVO<sub>4</sub> crystal,  $dn/dT$  are the thermal-optic coefficients of  $n$ ,  $\alpha_T$  is the thermal expansion coefficient along the  $a$  axis,  $l$  is the crystal length, and  $\omega_p(z)$  is the pump size in the active medium. With the usual  $M^2$  propagation law, the pump beam is given by

$$\omega_p^2(z) = \omega_{p0}^2 \left\{ 1 + \left[ \frac{\lambda_p M_p^2}{n\pi \omega_{p0}^2} (z - z_0) \right]^2 \right\}, \quad (3)$$

where  $\omega_{p0}$  is the radius at the waist,  $\lambda_p$  is the pump wavelength,  $M_p^2$  is the pump beam quality factor, and  $z_0$  is the focal plane of the pump beam in the active medium. The first and second terms in parentheses in Eq. (2) arise from thermal dispersion and axial strain, respectively. With the following parameters of the Nd:YVO<sub>4</sub> crystal:  $dn/dT = 3.0 \times 10^{-6}/\text{K}$ ,  $n = 2.165$ , and  $\alpha_T = 4.43 \times 10^{-6}/\text{K}$ , the relative contributions of thermal dispersion and axial strain can be found to be approximately 1:3.

With the thermal lens, the beam waist at the input face of the laser crystal is given by

$$\omega_l = \sqrt{\frac{\lambda}{\pi}} \frac{(Lf_{\text{th}})^{1/4}}{(1 - L/f_{\text{th}})^{1/4}}, \quad (4)$$

$$L = L^* + l(1/n - 1) + l_{\text{KTP}}(1/n_{\text{KTP}} - 1) + l_Q(1/n_Q - 1), \quad (5)$$

where  $L^*$  is the cavity length,  $l_{\text{KTP}}$  is the length of the KTP crystal,  $n_{\text{KTP}}$  is the KTP crystal's refractive index for the output laser beam,  $l_Q$  is the length of the Q-switched crystal, and  $n_Q$  is the refractive index of the Q-switched crystal for the output laser beam.

Figure 2 shows the dependence of the mode size on the pump power in 0.5-at. % Nd:YVO<sub>4</sub> crystal for several cavity lengths. The experimental data were measured by the knife-edge method. The theoretical results were calculated for the following parameters:  $\xi = 0.24$ ,  $K_c = 0.0523 \text{ W/K cm}$ ,  $\omega_{p0} = 0.2 \text{ mm}$ ,  $M_p^2 \approx 310$ ,  $n = 2.165$ ,  $n_{\text{KTP}} = 1.75$ ,  $n_Q = 2.33$ ,  $l = 6 \text{ mm}$ ,  $l_{\text{KTP}} = 20 \text{ mm}$ ,  $l_Q = 20 \text{ mm}$ ,  $dn/dT = 3.0 \times 10^{-6}/\text{K}$ , and  $\alpha_T = 4.43 \times 10^{-6}/\text{K}$ . The good agree-

ment between theoretical results and experimental data indicates that the thermal lens effect provides a stability mechanism in the present cavity. It is clear from Fig. 2 that the mode-to-pump size ratio is approximately 0.8–1.0 at  $L^* = 60 \text{ mm}$  for pump powers in the range of 5–20 W, leading to optimal mode matching. It should be noted that nearly 30–40% of the backward green light incident upon the Nd:YVO<sub>4</sub> is absorbed. Nevertheless, numerical calculations show that the forward green light almost dominates the output power. I also measured the fractional thermal loading by using the previous method<sup>11</sup> and confirmed that the absorbed green power does not result in a substantial contribution to the thermal loading beyond the quantum defect.

Figure 3 illustrates the average green output power at a repetition rate of 50 kHz at  $L^* = 60 \text{ mm}$  as a function of the incident pump power for several Nd:YVO<sub>4</sub>

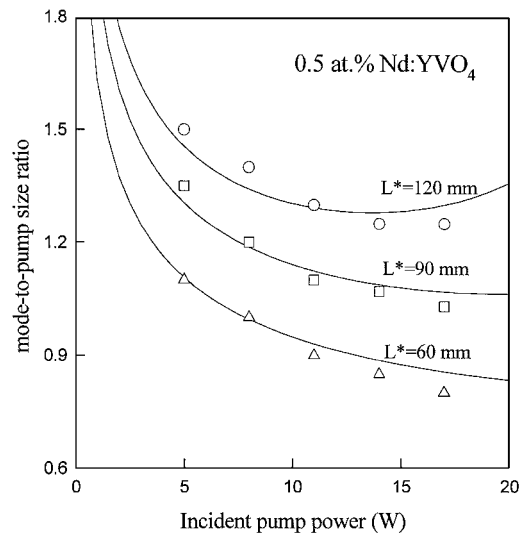


Fig. 2. Dependence of the mode-to-pump size ratio on the incident pump power for several cavity lengths: symbols, experimental data; curves, theoretical calculations.

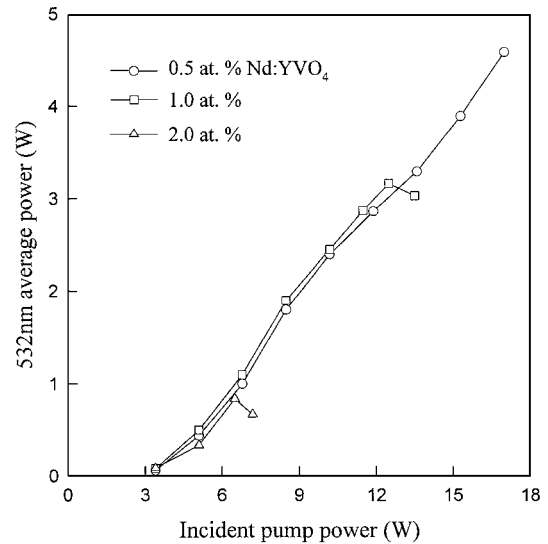


Fig. 3. Average green output power at a 50-kHz pulse-repetition rate as a function of the incident pump power for several Nd:YVO<sub>4</sub> crystals with different dopant concentrations.

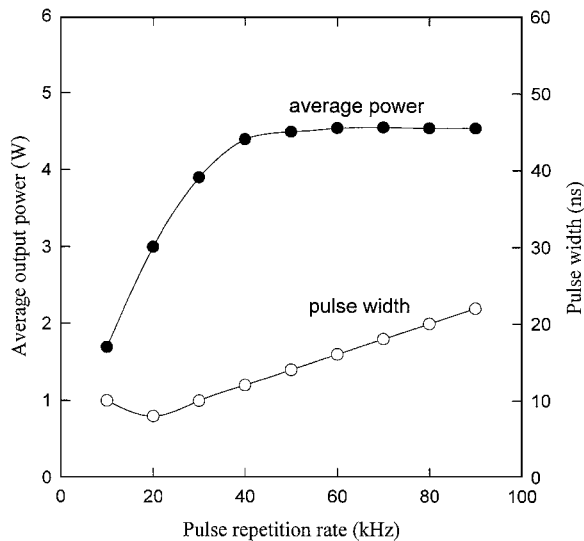


Fig. 4. Average green output power and pulse width as a function of the  $Q$ -switched pulse-repetition frequency.

crystals with different dopant concentrations. Experimental results show that, once the pump power reached the thermal fracture limit, the output power immediately dropped, and output characteristics were not reproducible when the pump power was decreased. As expected, the lower the dopant concentration (absorption coefficient), the higher the fracture-limited pump power. A maximum green output power of 4.6 W was obtained in a 0.5-at. % Nd:YVO<sub>4</sub> crystal at 17 W of absorbed pump power. To my knowledge, these are the highest efficiency and the highest power ever reported for a singly end-pumped  $Q$ -switched Nd:YVO<sub>4</sub>/KTP green laser.

Figure 4 shows the average green output power and laser pulse width at 17 W of pump power as a function of the pulse-repetition rate. To avoid damage to the intracavity optical components, I operated the  $Q$  switcher above 10 kHz. It can be seen that at low pulse-repetition rates the pulse width is short and the energy per pulse is high, whereas at higher pulse-repetition rates the energy per pulse is low and the pulse width is long but the average power is high. At full pump power, the pulse width increases from 8 ns at 20 kHz to 22 ns at repetition rates greater than 90 kHz. Previously, Hemmati and Lesh<sup>3</sup> reported a 3.5-W  $Q$ -switched intracavity frequency-doubled Nd:YAG/KTP green laser at a 50-kHz pulse-repetition rate. The pulse width in their research increased from 20 ns at 16 kHz to 52 ns at 60 kHz. The pulse width in the present green laser is  $\sim 2.5$  times shorter than the output results demonstrated by Hemmati and Lesh, mainly because of the compactness of the present cavity. Although the pulse energy in the Nd:YVO<sub>4</sub>/KTP laser is less than that in the Nd:YAG/KTP laser at frequency-repetition rates below 20 kHz, the shorter pulse width of the present design leads to a peak power that is nearly the same as that in the Nd:YAG/KTP laser. For frequency-repetition rates greater than 20 kHz, the output performance of the present system is generally better than that of the Nd:YAG/KTP system because of higher conversion.

After the optical elements were thermally stabilized, the fluctuations of the average power over hours of operation were measured to be  $\pm 4\%$ . No damage or darkening of the KTP crystal was observed in these experiments, and the laser performance was reproducible on a day-to-day basis. I measured the 1064-nm power leakage of the laser to estimate the intracavity peak power of the fundamental light. The 1064-nm output power was approximately 20–40-mW at 10–50-kHz repetition rates with 17-W pump power. For theoretical estimation, the intracavity peak power of the fundamental light was near 50–150 MW/cm<sup>2</sup>. These power levels are essentially below the optical damage threshold of the KTP crystal, which is usually  $>450$  MW/cm<sup>2</sup> for 10-ns pulses at 1064-nm. The beam quality factor at the maximum output power was  $\sim 2.0$ . The degradation of the beam quality arises mainly from the thermally induced aberration. I believe that a composite crystal structure,<sup>6</sup> which is fabricated by diffusion bonding of a doped crystal to an undoped piece of the same cross section, can be used to reduce the thermally induced distortion. Use of the composite crystal with the present cavity is currently under way.

I have demonstrated the use of a thermal lens to obtain high efficiencies of  $Q$ -switched green output power with a fiber-coupled laser diode. The cavity is formed by a coated Nd:YVO<sub>4</sub> crystal, an acousto-optical  $Q$  switcher, and a coated KTP crystal. With the thermally induced lens, the cavity length was adjusted to yield the optimal mode-to-pump size ratio for the maximum output power. The strategy for avoiding the thermally induced fracture was to use a YVO<sub>4</sub> crystal of lower Nd concentration. 4.6 W of 532-nm average power at a repetition rate of 50 kHz was generated with a 17-W pump power, corresponding to a conversion efficiency of 27%. The present result indicates that there is substantial scope for further power scaling of end-pumped Nd:YVO<sub>4</sub> lasers with low Nd concentrations.

The author's e-mail address is yfchen@cc.nctu.edu.tw.

## References

1. V. G. Ostroumov, F. Heine, S. Kück, G. Huber, V. A. Mikhailov, and I. A. Shcherbakov, *Appl. Phys. B* **64**, 301 (1997).
2. T. Taira and T. Kobayashi, *IEEE J. Quantum Electron.* **30**, 800 (1994).
3. H. Hemmati and J. R. Lesh, *Opt. Lett.* **17**, 1322 (1994).
4. N. Mackinnon and B. D. Sinclair, *Opt. Commun.* **105**, 183 (1994).
5. Y. F. Chen, *IEEE Photon. Technol. Lett.* **9**, 669 (1998).
6. M. Tsunekane, N. Taguchi, T. Kasamatsu, and H. Inaba, *IEEE J. Sel. Top. Quantum Electron.* **3**, 9 (1997).
7. Y. F. Chen, *IEEE J. Quantum Electron.* **35**, 234 (1999).
8. J. J. Zayhowski and A. Mooradian, *Opt. Lett.* **14**, 1989 (1989).
9. G. J. Dixon, L. S. Lingvay, and R. H. Jarman, *Proc. SPIE* **1104**, 107 (1989).
10. C. Pfistner, R. Weber, and H. P. Weber, *IEEE J. Quantum Electron.* **30**, 1605 (1994).
11. Y. F. Chen and H. J. Kuo, *Opt. Lett.* **23**, 846 (1998).